Research Article

Encapsulation of Sorbitan Ester-Based Organogels in Alginate Microparticles

Sai S. Sagiri,[1] Kunal Pal,[1,5] Piyali Basak,[2] Usman Ali Rana,[3] Imran Shakir,[3] and Arfat Anis[4]

Abstract. Leaching of the internal apolar phase from the biopolymeric microparticles during storage is a great concern as it undoes the beneficial effects of encapsulation. In this paper, a novel formulation was prepared by encapsulating the sunflower oil-based organogels in alginate microparticles. Salicylic acid and metronidazole were used as the model drugs. The microparticles were prepared by double emulsion methodology. Physico-chemical characterization of the microparticles was done by microscopy, FTIR, XRD, and DSC studies. Oil leaching studies, biocompatibility, mucoadhesivity, *in vitro* drug release, and the antimicrobial efficiency of the microparticles were also performed. The microparticles were found to be spherical in shape. Gelation of the sunflower oil prevented leaching of the internal phase from the microparticles. Release of drugs from the microparticles followed Fickian kinetics and non-Fickian kinetics in gastric and intestinal environments, respectively. Microparticles showed good antimicrobial activity against both Gram-positive (*Bacillus subtilis*) and Gram-negative (*Escherichia coli*) bacteria. The results suggested that the developed formulations hold promise to carry oils without leakage of the internal phase. Encapsulation of organogels within the microparticles has improved the drug entrapment efficiency and improved characteristics for controlled delivery applications.

KEY WORDS: alginate; drug delivery; leaching; microparticles; organogels.

INTRODUCTION

Encapsulation of oils (*e.g.*, neem oil, fish oil, wheat germ oil, evening prime rose oil, and citronella oil) within polymeric microparticles has been extensively studied for food, pharmaceutical, and nutraceutical applications. One of the main advantages of encapsulation of oil is the conversion of the apolar liquid (*e.g.*, oil) into solid dosage forms which, in turn, facilitates easy transportation and handling (1). In addition to this, encapsulation also allows taste and/or odor masking of the active ingredients present in the oil phase. The stability of the active ingredients may also be increased to a great extent (2). The main problem associated with the encapsulation of oils within microparticles is the leaching of the internal (oil) phase during stor-age. The leaching of the internal phase undoes the main advantages of the encapsulation and subsequently reduces the encapsulation efficiency. To solve the problem, researchers have used different approaches. The widely used approach is to encapsulate the oil in blended polymers (3). Another approach is by adopting complex protocols for the preparation of microparticles (4). In the present study, we propose a novel and simple method to improve these shortcomings by immobilizing the internal oil phase using liquid polysorbate-based gelators. The process of gelation of oil/organic solvent using suitable gelator molecules is regarded as organogelation, and the structured formulation is known as oleogels (often regarded as organogels on a broader sense). Organogels are defined as the semi-solid formulations which contains oil/apolar phase as the continuous phase, which is immobilized in a 3D network of gelator molecules (organogelators). Our group has previously reported the development of span 80-tween 80 (liquid polysorbates)-based sunflower oil organogel (5). All the components used in this study are generally regarded as safe (GRAS) materials and FDA approved for oral administration (6, 7).

To establish our hypothesis that the gelation of the internal phase might reduce the leaching of the internal phase, attempts have been made to encapsulate span 80-tween 80-based sunflower oil organogels. Blank microparticles (microparticles without any internal phase) and microparticles with sunflower oil served as controls. Salicylic acid and metronidazole were used as model drugs. The biocompatibility, mucoadhesivity, *in vitro* drug release, and

[1] Department of Biotechnology and Medical Engineering, National Institute of Technology, Rourkela 769008, India.
[2] School of Bioscience & Engineering, Jadavpur University, Kolkata 700032, India.
[3] Deanship of Scientific Research, College of Engineering, King Saud University, Riyadh 11421, Saudi Arabia.
[4] Department of Chemical Engineering, King Saud University, Riyadh 11421, Saudi Arabia.
[5] To whom correspondence should be addressed. (e-mail: pal.kunal@yahoo.com)

the antimicrobial efficiency of the microparticles were determined.

MATERIALS AND METHODS

Materials

Sodium alginate, calcium chloride (fused), calcium carbonate, potassium dihydrogen phosphate, span 80-tween 80, and dialysis tubing (MW cutoff: 12–14 kDa) were purchased from Himedia, Mumbai, India. Glacial acetic acid and hydrochloric acid were purchased from Merck, Mumbai, India. Food-grade-refined sunflower oil (Fortune sunlite®, Adani Wilmar Ltd. Gujarath, India) was purchased from the local market. Salicylic acid was procured from Sara fine chemicals, Vadodhara, India, and metronidazole was received as a kind gift from Aarthi drugs Ltd., Mumbai, India. MG63 cell line was procured from NCCS, Pune, India. Fresh goat blood and freshly excised goat small intestine were collected in cold saline from the local butcher shop and were used within 1 h of collection. Double distilled water was used throughout the study.

Preparation of Span 80Tween 80-Based Organogels

The organogels were prepared as described by our group elsewhere (5). In brief, 5.25 g of the surfactant mixture (span 80:tween 80 ratio of 1:2 *w/w*) and 1.25 g of sunflower oil were mixed to form a homogenous solution at room temperature (25°C). To this, 3.25 g of water was added drop by drop with continuous mixing. The homogeneous mixture was allowed to settle at room temperature to form organogel. The prepared organogel was labeled as "OG" and used for further studies. To prepare the drug containing organogels, either 1% (*w/w*) salicylic acid or metronidazole was dissolved in sunflower oil and water, respectively. The drug containing oil and aqueous phases were used to prepare salicylic acid and metronidazole containing organogels, respectively. The method of preparation of drug containing organogels was the same as mentioned earlier. Salicylic acid and metronidazole containing organogels were labeled as OGSA and OGMZ, respectively.

Preparation of Microparticles

The microparticles were synthesized by modified double emulsion method or internal gelation method (5). Briefly, 0.5 g of sodium alginate was dissolved in 20 g of water and kept on stirring at 250 rpm at room temperature. After complete dissolution of the sodium alginate, 0.4 g of calcium carbonate was added and homogenized at 250 rpm. Then, a mixture of 0.5 g of span 80 and 5 g of internal oil phase was added and further homogenized for 15 min to form an oil-in-water emulsion. The internal phase was either sunflower oil or organogel. The emulsion was further homogenized in an ice bath for 10 min to form a thick emulsion. The thick emulsion, so obtained, was transferred to 60 ml of ice-cold sunflower oil (external phase) and homogenized for 5 min at 250 rpm to form a double emulsion. After the homogenization, 5 ml of acidified oil (4.5 ml sunflower oil + 0.5 ml glacial acetic acid) was added to the external phase of the double emulsion (which is under stirring) to induce ionic crosslinking and

gelation of the alginate layer to form microparticles. The microparticles were washed with 0.5 M calcium chloride solution containing 1% (*v/v*) tween 80, followed by washing with water. The microparticles with OG and sunflower oil as the internal phases were labeled as MOG and MSO, respectively. The microparticles without any internal phase (*i.e.*, OG or sunflower oil) were labeled as blank microparticles or BM. Drug containing microparticles were also prepared as described above, but the internal phases of microparticles were changed with drug containing internal phases. During the preparation of drug formulations, internal phase, OG was replaced with either OGSA or OGMZ. The microparticles with OGSA and OGMZ were labeled as MOGSA and MOGMZ, respectively. Similarly, sunflower oil was replaced with 1% (*w/w*) salicylic acid or metronidazole containing sunflower oil as the internal phase and was labeled as MSOSA or MSOMZ, respectively. Drug containing blank microparticles were also prepared as controls of the study. In this regard, 1% (*w/w*) of either salicylic acid or metronidazole was dispersed in sodium alginate solution and then the microparticles were synthesized. Salicylic acid and metronidazole containing blank microparticles were labeled as BMSA and BMMZ, respectively. The prepared microparticles were stored at 4°C until further use.

Microscopy

The microstructure of the microparticles was observed under an upright bright-field microscope (LEICA-DM 750 equipped with ICC 50-HD camera, Germany). The size distribution of the microparticles (sample size ~1,000) was determined using NI Vision Assistant-2010 software (8). The size distribution was estimated by calculating SPAN factor (size distribution factor) and percentage coefficient of variation (%CV) (8).

$$\text{SPAN} = (d_{90} - d_{10})/d_{50} \tag{1}$$

$$\%\text{CV} = \left[\frac{\text{Standard deviation}}{\text{Mean}}\right] \times 100 \tag{2}$$

where, d_{90}, d_{50}, and d_{10} are the diameters of the 90, 50, and 10% of the microparticles population.

Scanning electron microscope (JEOL, JSM-6390, Japan) was used to study the topology of the microparticles. The microparticles were dried at 40°C for overnight and sputter coated with platinum before analysis.

Leaching Studies

The microparticles were wiped with filter paper to remove the surface-bound moisture and traces of external oil, if any. Of the microparticles, 0.5 g was accurately weighed and kept on a fresh filter paper and incubated at 37°C (9). The leakage of internal oil phase was monitored for 2 h.

For quantitative analysis of leaching, another method was adopted (10). In short, accurately weighed 0.1 g (W_1) of microparticles was soaked in 1.0 ml (W_2) of double distilled water for 1.0 h at 37°C in a microcentrifuge tube. After

incubation, the tubes were centrifuged at 10,000 rpm for 2 min (SPINWIN, MC-02, Tarsons, India). The pellet (W_3) and the supernatant (W_4) were weighed separately and then dried at 55°C for 48 h. Subsequently, the dried pellet (W_5) and supernatant (W_6) were weighed again.

The swelling power of the microparticles was calculated as follows:

$$\text{Swelling power} = \frac{W_3}{W_5} \tag{3}$$

The percentage of leaching from the microparticles was calculated as follows:

$$\%\text{leaching} = \frac{W_6}{W_1} \times 100 \tag{4}$$

Mechanical Analysis

The apparent viscosity of the primary emulsions of the microparticles was determined by using rotational cone and plate viscometer (BOHLIN VISCO-88, Malvern, UK). The cone angle and diameter are 5.4° and 30 mm, respectively. A gap of 0.15 mm was maintained between the cone and the plate throughout the study. The analysis was performed by varying the shear rate from 15 to 95 s^{-1} at room temperature.

Cohesiveness of the primary emulsions was predicted by performing compressive analysis *via* backward extrusion studies using texture analyzer (Stable Microsystems, TA-HDplus, UK). Analysis was performed by moving the probe at a speed of 1 mm s^{-1} to a 20-mm distance within the emulsion and returned to the original position at the same speed. The experiment was performed in auto-force mode with a trigger force of 3 g.

Drug Encapsulation Efficiency

Of the dried microparticles containing drugs, 0.5 g was triturated in 50 ml of pure methanol and filtered through Whatmann filter paper (Sartorius stedim, grade: 389) (8). Presence of drug in the filtrate was checked using UV-visible spectrophotometer (UV-3200, Labindia, Mumbai, India) at 294 and 321 nm for salicylic acid and metronidazole, respectively. Drug encapsulation efficiency was calculated and reported as percentage drug encapsulation efficiency (%DEE) given by Eq. 3 (11).

$$\%\text{DEE} = \left[\frac{\text{Practical loading}}{\text{Theoritical loading}} \right] \times 100 \tag{3}$$

Molecular Interaction Studies

The chemical interactions among the components of the formulations were studied using Fourier transform infrared (FTIR) spectrophotometer with attenuated total reflection (ATR) mode (alpha-E, Bruker, Germany) in the wave number range of 4,000 to 500 cm^{-1}. As the analysis was performed in ATR mode, pure microparticles were used without any further processing. Dried microparticles were loaded upon the zinc selenide (ZnSe) crystal of the spectrophotometer, and scanning was performed for 24 times.

The X-ray diffraction analysis of the microparticles was also carried out using the pure dried microparticles without any processing. The microparticles were coated as a layer upon a clean glass slide and then studied using X-ray diffractometer (PW3040, Philips Analytical ltd., Holland). The instrument uses monochromatic Cu K_α radiation ($\lambda = 0.154$ nm) for analysis. The scanning was done in the range of 5° 2θ to 50° 2θ at a scanning rate of 2° 2θ/min.

Thermal Studies

Thermal analysis of the microparticles was carried out using differential scanning calorimeter (DSC-200F3 MAIA, Netzsch, Germany) at a scanning rate of 1°C/min under inert nitrogen atmosphere (flow rate 40 ml/min). Thermal properties of the microparticles (5 to 15 mg) were analyzed in aluminum crucibles.

Biocompatibility and Physical Interaction Studies

The cytocompatibility of the microparticles was determined using MG63 cell line by solvent extraction method. In short, 1 g of the sample was put into the dialysis tubing and was subsequently dipped into 25 ml of phosphate buffer saline. Of the leachate, 200 μl was added to a well of a 96-well plate. The plate was previously seeded with 5×10^4 cells and subsequently incubated (37°C, 5% carbon dioxide) for 12 h to allow adherence of the cells. After the addition of the leachate, the plate was further incubated for 48 h. After incubation, the cell viability was assessed using MTT assay (12).

Physical interaction studies were carried out by mucoadhesivity and swelling equilibrium studies. Mucoadhesivity of the microparticles was analyzed by *in vitro* wash-off method (11). Briefly, small intestine of goat was longitudinally cut open, washed thoroughly with saline, and cut into pieces of 2×2 cm^2. The outer surface of the intestine was attached onto a glass slide using acrylate adhesive. This exposed the internal surface (mucosal layer) of the intestine. Of the microparticles, 0.2 g was weighed and placed over the mucosal surface. A 5-g weight was applied over the microparticles for 1 min to adhere the microparticles. The slides were subsequently put vertically into the United States Pharmacopeia (USP) disintegration apparatus containing 900 ml of the phosphate buffer (pH=7.2) at 37°C. The time required for detaching the microparticles from the mucosal surface was noted down.

In Vitro Drug-Release Studies

The release of the drugs from the drug-loaded microparticles was studied under *in vitro* conditions at different pHs. The studies were carried out at gastric (pH=1.2) and intestinal (pH=7.2) environments. Hydrochloric acid buffer of pH 1.2 and phosphate buffer of pH 7.2 were used for this study. Accurately weighed (~1 g) dried microparticles were placed in a dialysis membrane bag. The bag was tightened from both ends and subsequently submerged in 50 ml of buffer. Formation of saturation layer at the interface of the dialysis

membrane and the dissolution medium was prevented by keeping the buffer under stirring at 100 rpm. The experiment was conducted at 37°C. The buffer was replaced with fresh buffer at regular intervals of 30 min. The experiment was conducted for a period of 12 h. Quantification of the released drug was done by analyzing the samples at 294 and 321 nm for salicylic acid and metronidazole, respectively. The statistical analysis of the results was performed using MINITAB 14.1 software.

Bioactivity of the drugs after being released from the microparticles was tested by antimicrobial studies. The antimicrobial efficiency was tested against *Bacillus subtilis* (MTCC 121) and *Escherichia coli* (NCIM 5051). The antimicrobial studies were carried out by direct contact assay method (13). Briefly, ~1 g of the drug-loaded-dried microparticles was dispersed in 100 ml of autoclaved nutrient broth containing bacterial inoculum (1 ml of 10^6 cfu/ml). The nutrient broth was incubated at 37°C in a shaker incubator, operated at 120 rpm. Under aseptic conditions, 1 ml of the nutrient broth was collected at an interval of 1 h, and the growth of the bacteria was measured at 595 nm using UV-visible spectrophotometer. Microparticles without drug were served as negative control.

RESULTS AND DISCUSSION

Preparation of Span 80-Tween 80-Based Organogels

Organogels were prepared using a mixture of non-ionic surfactants of span 80-tween 80 (1:2 *w/w*) as an organogelator. Drop-wise addition of water to the homogeneous mixture of sunflower oil and surfactant mixture resulted in the formation of a white turbid emulsion. The addition of water results in the exothermic reaction, which results in the increase in the temperature of the emulsion to ~40°C. The release of energy during preparation of the organogel indicates that the organogels attain a lower energy state. Hence, it is expected that the prepared organogel will be thermodynamically stable in nature. The emulsion, so formed, was vortexed and allowed to cool at room temperature to form a white-colored gel. The gelation was confirmed by inverted tube method (Fig. 1) (14). The stability and characterization of the organogels has been well described in our previous study (5). Salicylic acid- and metronidazole-loaded gels were also found to be stable at room temperature. The composition of organogels was listed in Table I.

Preparation of Microparticles

The composition of the internal phase of the microparticles has been listed in Table II. Primary emulsions were prepared by dispersing either sunflower oil or organogel in alginate solution. Addition of the primary emulsion to the external phase sunflower oil resulted in the formation of oil-in-water-in-oil multiple emulsion. Acidification of the external oil phase using acidified oil resulted in the release of calcium ions from calcium carbonate, present in the alginate layer. The calcium ions were responsible for crosslinking of the alginate present within the aqueous phase of the multiple emulsions (5). This resulted in the solidification of the alginate layer as spherical particles, which in turn, immobilized the

internal phase of the multiple emulsions. The external oil phase was removed by washing the particles thoroughly. In a similar way, salicylic acid and metronidazole containing microparticles were also prepared.

Microscopy

The microparticles have shown distinct variation in their internal structure (Fig. 2). BM was semi-transparent due to the absence of any internal phase within the microparticles. MSO showed multiple cores indicating that MSO was a multi-core microparticle rather than a single-core microparticle. The core of the microparticles was globular in nature suggesting the entrapment of sunflower oil within the alginate particles. MOG were more opaque than BM and MSO as was evident from the darker nature of the microparticles. This may be associated with the presence of the semi-solid organogel, which prevented the transmission of the light through the microparticles (13).

The average diameter of the microparticles (sample size ~1,000) was found to be highest for MOG followed by MSO and BM. Analysis suggested that MOG had a broad size distribution over MSO and BM (Fig. 2g, h). Polydispersity of the microparticles was expressed in terms of SPAN factor. In general, SPAN factor <2.0 and d_{50}<10 μm suggest narrow size distribution (9). The SPAN factors of the microparticles were <2.0, but the d_{50} were >10 μm (Fig. 2i). Higher d_{50} values may be due to the method of microparticle fabrication. In general, ionotropic gelation method results in the formation of microparticles having sizes in between 10 and 400 μm (9). Keeping these facts in mind, the size distribution of the microparticles may be regarded as narrow. %CV was calculated from the particle size distribution graph. A higher value of %CV was observed for MOG. This may be associated with the physical nature of the internal phase. The apparent viscosities of the alginate emulsions were less viscous in BM and MSO as compared to the MOG. This resulted in the formation of larger particles of wide size distribution in MOG followed by MSO and BM.

SEM studies suggested that the microparticles are circular but are having polydispersity (Fig. 2). The sizes of the microparticles were smaller as compared to the particle size obtained from light microscopy. This is due to the fact that the microparticles for SEM analysis were completely dried. The evaporation of water has lead to the shrinkage of the microparticles which resulted in loss of spherical nature to a certain extent. The extent of loss of sphericity was more in BM and MSO as compared to MOG. The microscopic studies indicated that the physical nature of the internal phase was affecting the appearance of the microparticles.

Leaching Studies

Leaching of internal phase from the MSO showed a darker region surrounding the microparticles (Fig. 3). This indicated that sunflower oil was leaking out of the microparticles. On the other hand, MOG did not show any signs of leakage until the end of the experiment (2 h). This may be attributed to the gelation of the sunflower oil due to which apparent viscosity was increased (15). The difference in apparent viscosity of the primary emulsions of microparticles
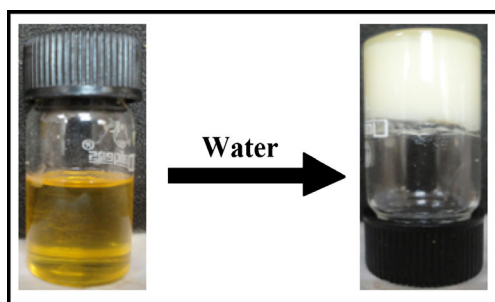
Fig. 1. Formation of stable organogels

and pure alginate solution was found by using Bohlin viscometer (Fig. 3). The apparent viscosity of MOG's primary emulsion was found to be higher than that of MSO and pure alginate solution. The difference in apparent viscosities can be explained by the internal phase associated with them. Presence of organogel in the alginate solution of MOG has yielded higher apparent viscosity. Since fatty acyl organogels have the tendency to accommodate water within their gelator network, the organogels might have absorbed some amount of water (16). This might have resulted in the increase in viscosity of the emulsion. As gelator network is absent in the emulsion of MSO, its apparent viscosity was lower than that of the emulsion of MOG. In addition to the differences in apparent viscosity of the emulsions, the textural properties of the emulsions were also identified. Cohesiveness of the emulsions was determined by performing backward extrusion studies. The area under the positive curve (during forward movement of the probe) indicates the cohesiveness of the emulsions (represented by dotted lines) (17). The results suggested that the cohesiveness of the emulsions is following the similar trend as that of apparent viscosity (MOG > MSO > BM) (BM 0.15 kg s^{-1}; MSO 0.16 kg s^{-1}; MOG 0.2 kg s^{-1}). This indicates that the increase in viscosity of MOG's emulsion is due to the increase in cohesiveness among their components. Viscometric and textural (backward extrusion) studies suggested that the addition of organogel to the alginate solution has enhanced the apparent viscosity and cohesiveness of the alginate solution. The increase in viscosity might have prevented the leaching of the internal phase. This study shows that the leakage of oil from microparticles may be overcome by inducing gelation of the internal phase.

Leaching of oil from the microparticles was quantified by performing another method, and the results were shown in Fig. 3. MSO showed 46.1% of oil leaching, whereas MOG showed 9.4% of leaching. This suggests that the presence of organogel has prevented the leaching of sunflower oil from

the microparticles. Quantification of leachate confirms the efficiency of organogels in preventing the oil leaching from alginate microparticles. In addition to the quantification of leachate, this study has enabled to calculate swelling power. Swelling power of the microparticles seems to be unaffected by their internal phase (Fig. 3). Moreover, similar swelling power is may be due to the presence of equal concentration of sodium alginate in the microparticles.

Drug Entrapment Efficiency

The percentage of drug encapsulation efficiency (%DEE) of microparticles was varying with nature of the internal phase (Table III). The lowest %DEE of BM may be associated with the absence of the internal phase. Drugs might have diffused out of the porous alginate microparticles by diffusion during the preparation of the microparticles (15). The %DEE of MSO was slightly better than that of BM and may be associated with the partitioning effect. The %DEE was highest in MOG which may be due to the combined effect of partitioning and increased viscosity of the internal phase. The semi-solid organogels might have restricted the diffusion of drugs and resulted in higher %DEE.

Molecular Interaction Studies

The FTIR spectra of the microparticles showed peaks corresponding to calcium alginate (Fig. 4). Figure 4a shows a spectral band at ~3,600 to 3,050 cm^{-1} with a maximum intensity at ~3,370 cm^{-1}. The band at ~3,370 cm^{-1} was due to the stretching vibrations of hydrogen-bonded OH groups (18). The peaks at ~1,410 and ~1,600 cm^{-1} might be associated with the symmetric and asymmetric stretching vibrations of the COO^{-}, respectively, while the presence of the three peaks in the range of 1,200–950 cm^{-1} may be attributed to the presence of the carbohydrate backbone (19). The peak at ~3,370 cm^{-1} was broadened and shifted toward lower wave numbers in MSO and MOG, suggesting an increase in hydrogen bonding (20).

The drug containing microparticles showed characteristic peaks of salicylic acid and metronidazole, in addition to the peaks associated with calcium alginate. Salicylic acid containing microparticles have shown distinct peaks at ~1,600 cm^{-1} (C=C bond of aromatic ring), 1,666 and 1,649 cm^{-1} (C=O stretching of COOH), and 756 and 719 cm^{-1} (C–H out of plane bending in the phenol substitution ring) indicating the presence of salicylic acid (21). The peaks at 1,238 cm^{-1} (ester carbonyl peak), 1,747 cm^{-1} (carbonyl stretching), and 1,593 cm^{-1} (asymmetric nitro stretch), associated with

Table I. Composition of the Organogels

Sample	Surfactant mixture (% w/w)	Sunflower oil (% w/w)	Water (% w/w)	Salicylic acid (% w/w)	Metronidazole (% w/w)
OG	52.5	12.5	32.5	–	–
OGSA	52.5	12.5	31.5	1.0	–
OGMZ	52.5	12.5	31.5	–	1.0

OG organogel, *OGSA* salicylic acid containing organogel, *OGMZ* metronidazole containing organogel

Table II. The Internal Phase Composition of the Microparticles

Samples	Internal phase
BM	No internal phase
MSO	Sunflower oil
BMSA	Blank microparticles with 1% (w/w) salicylic acid
BMMZ	Blank microparticles with 1% (w/w) metronidazole
MSOSA	Sunflower oil containing 1% (*w*/*w*) salicylic acid
MSOMZ	Sunflower oil containing 1% (*w*/*w*) metronidazole
MOG	Organogel
MOGSA	Organogel containing 1% (*w*/*w*) salicylic acid
MOGMZ	Organogel containing 1% (*w*/*w*) metronidazole

BM blank microparticles, *MSO* microparticles with sunflower oil, *BMSA* salicylic acid containing blank microparticles, *BMMZ* metronidazole containing blank microparticles, *MSOSA* microparticles with salicylic acid containing sunflower oil, *MSOMZ* microparticles with metronidazole containing sunflower oil, *MOG* microparticles with organogel, *MOGSA* microparticles with organogel containing salicylic acid, *MOGMZ* microparticles with organogel containing metronidazole

metronidazole, were observed in metronidazole containing microparticles (22). Though the peaks of the drugs were conserved in the microparticles, the characteristic peaks of the alginate backbone (1,200–950 cm^{-1}) were shifted slightly toward a lower wave number. This suggested a strong association of the drugs with the components of the microparticles (21). At the same time, absence of any new characteristic peak in the spectra suggested that the drugs are in their native state, and there were no chemical interactions between the drugs and the microparticles.

The diffractogram of BM showed two peaks at 13.7° 2θ and 23° 2θ, whereas the diffractograms of MSO and MOG showed only one peak at 23° 2θ (Fig. 4c). The peak at 13.7° 2θ of BM was not visible in MSO and MOG. On the other hand, the peak at 23° 2θ was intensified. This may be due to the interactions among the alginate and the internal phase molecules, which resulted in the alteration in the molecular packing of the alginate molecules. The alteration in the molecular packing might have been associated with the formation of regular crystallites (18).

The drug containing microparticles showed feeble peaks associated with the drugs (Fig. 4d). This suggested that the physical nature of the drugs was not altered during encapsulation. Incorporation of the drugs within the microparticles has altered the intensity of the peak at 23° 2θ. This suggested
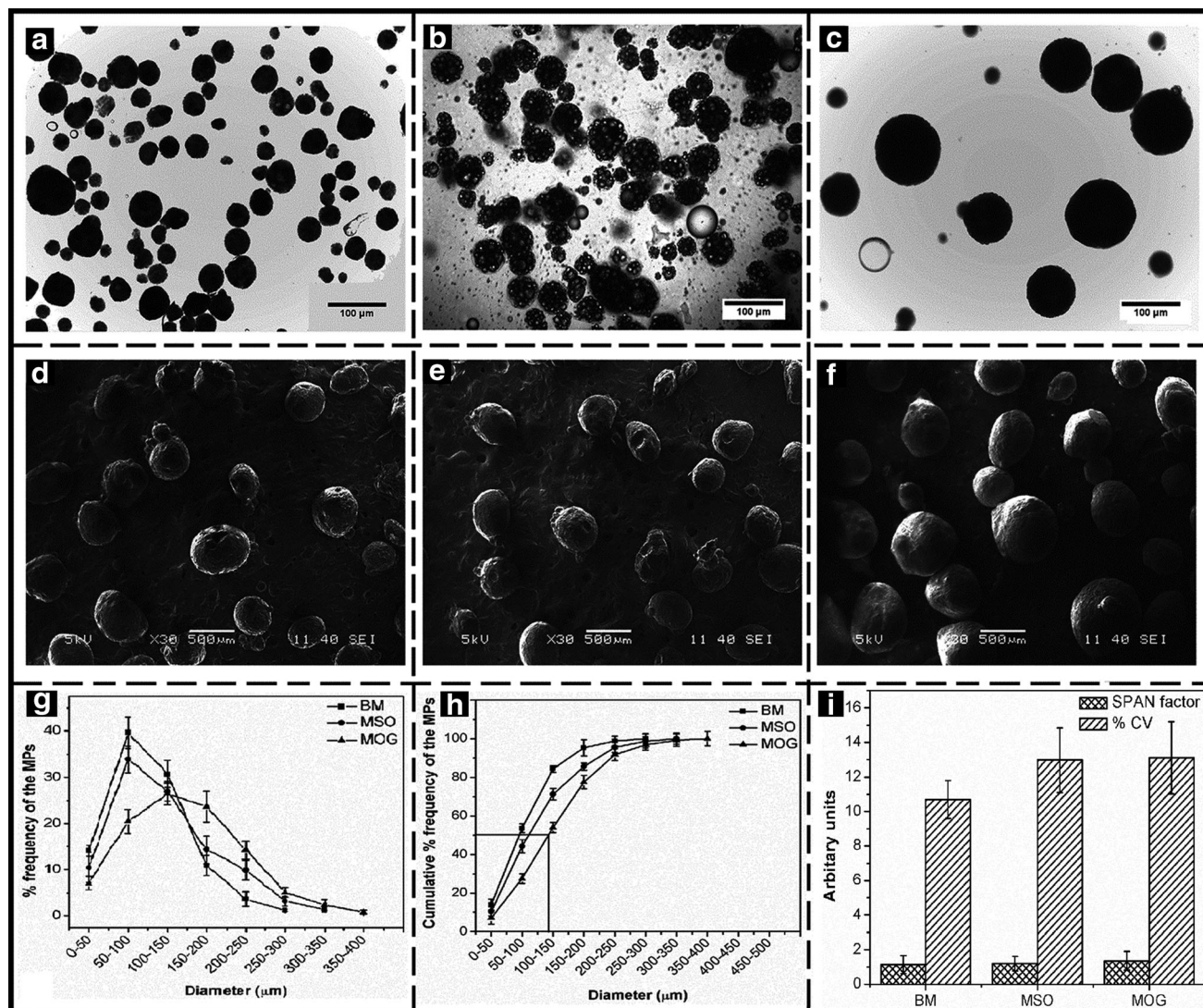

Fig. 2. Bright-field microscopic images: **a** BM, **b** MSO, and **c** MOG; SEM images: **d** BM, **e** MSO, and **f** MOG; and **g–i** size distribution analysis
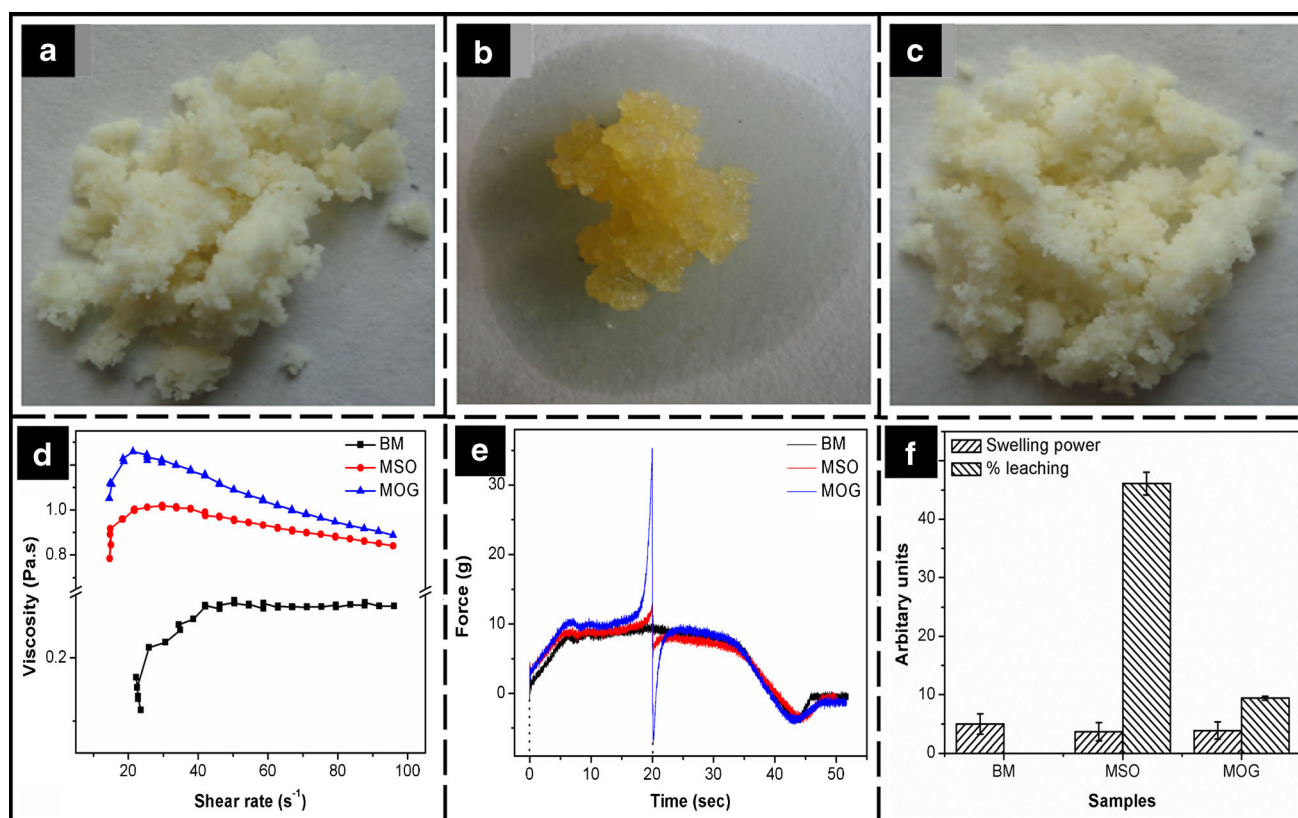
Fig. 3. Photographs showing **a** BM, **b** MSO **c** MOG microparticles after 2 h of leaching study, **d** Viscosity profile, **e** Backward extrusion profile of the primary emulsions of microparticles and **f** Swelling power and % leaching of microparticles

that the addition of salicylic acid and metronidazole have altered the molecular packing order of the alginate molecules to form regular crystallites (18). The results indicated an existence of good compatibility among the alginate, organogels, and drug molecules. This may be associated with the strong interactions (*e.g.*, hydrogen bonding) among the components of the microparticles, suggested by the FTIR studies (18).

Thermal Studies

Figure 5a shows the thermograms of the organogel and developed microparticles. The thermogram of sunflower oil

showed an endothermic peak at ~34°C. The organogel showed a broad endothermic peak at ~95°C. This is due to the combined effect of melting of the organogel and evaporation of water present in the organogel (18). BM showed an endothermic peak at ~100°C which may be attributed to the evaporation of the bound water associated with the alginate. Although dried microparticles were used, the thermal profile suggested that it was not possible to remove the bound water completely. Similar observations have also been reported earlier (23). MSO and MOG have shown endothermic peaks at ~60°C. This endothermic peak may be associated with the heating of sunflower oil. In our previous study, we have found that the gel to sol transition temperature of

Table III. %DEE and Drug Release Kinetics of the Microparticles

		Higuchi model		BL model		KP model			
		GB	IB	GB	IB	Gastric buffer (GB)		Intestinal buffer (IB)	
Sample	%DEE	R^2	R^2	R^2	R^2	n	Type of diffusion	n	Type of diffusion
BMSA	52±2.4	0.99	0.99	0.98	0.97	0.40	Fickian	0.50	Non-Fickian
MSOSA	58±3.1	0.99	0.99	0.97	0.98	0.51	Non-Fickian	0.51	Non-Fickian
MOGSA	81±2.4	0.99	0.97	0.99	0.99	0.52	Non-Fickian	0.59	Non-Fickian
BMMZ	44±2.7	0.99	0.98	0.96	0.96	0.42	Fickian	0.67	Non-Fickian
MSOMZ	49±2.5	0.99	0.97	0.97	0.99	0.55	Non-Fickian	0.78	Non-Fickian
MOGMZ	78±3.4	0.99	0.99	0.96	0.99	0.49	Non-Fickian	0.62	Non-Fickian

%DEE percentage drug encapsulation efficiency, *BL* Baker-Lonsdale, *KP* Korsmeyer-Peppas, *GB* gastric buffer, *IB* intestinal buffer, *BMSA* salicylic acid containing blank microparticles, *MSOSA* microparticles with salicylic acid containing sunflower oil, *MOGSA* microparticles with organogel containing salicylic acid, *BMMZ* metronidazole containing blank microparticles, *MSOMZ* microparticles with metronidazole containing sunflower oil, *MOGMZ* microparticles with organogel containing metronidazole
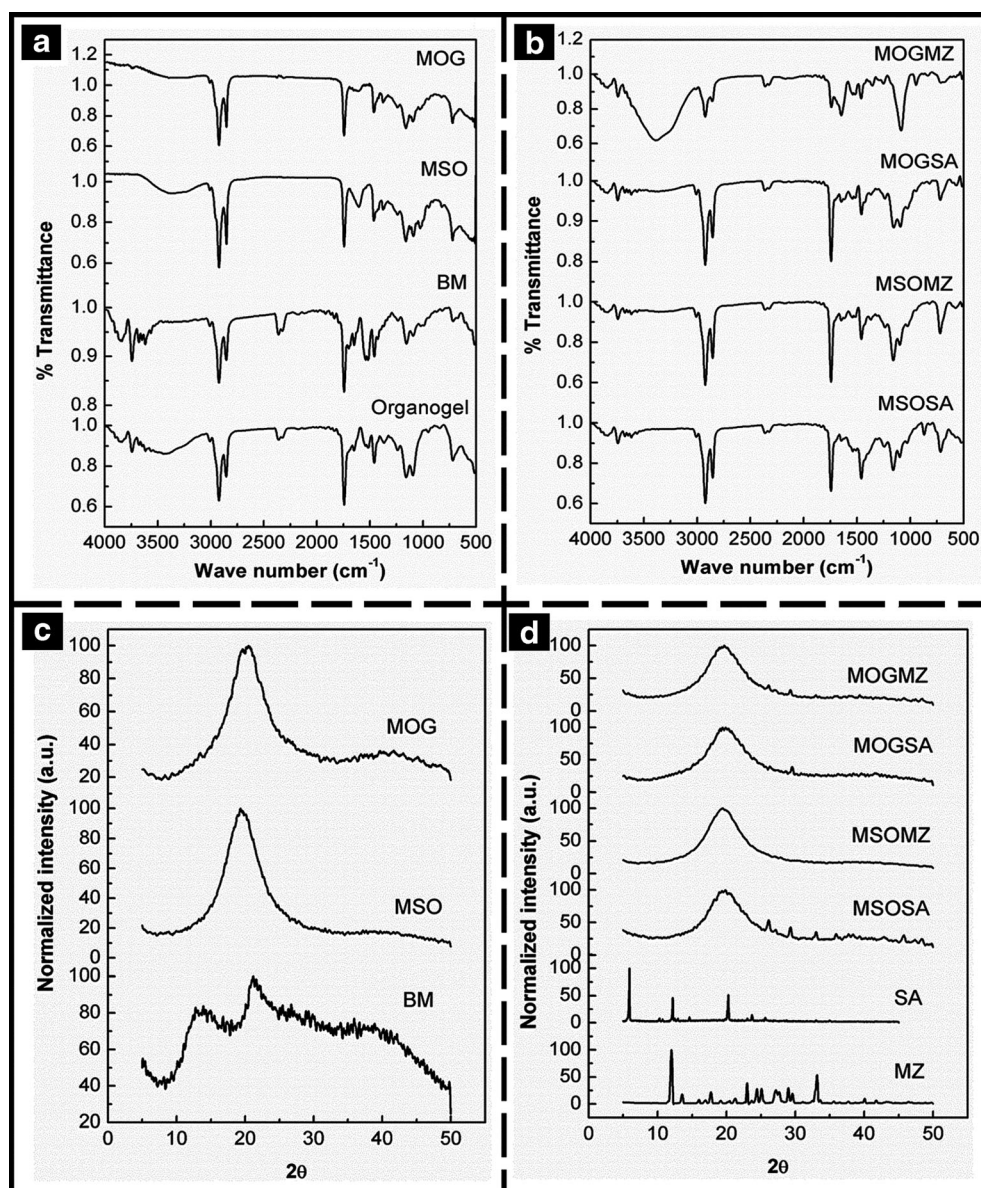
Fig. 4. a–b FTIR spectra and **c–d** XRD profiles of microparticles

the span 80-tween 80 organogels was found to be 55 to 70°C (5). The shift of the endotherm to the higher temperatures may be attributed to the increased crystalline nature of the microparticles (as was evident from the X-ray diffraction (XRD) studies). The endothermic peak of MOG was broader than that of MSO. This can be explained by the simultaneous evaporation of the water present in the organogel. Thermal analysis suggests that the organogels were successfully encapsulated within the microparticles.

Thermal analysis of the drug containing microparticles was tested in the temperature range of 30 to 300°C (Fig. 5b). Pure salicylic acid and metronidazole have shown endothermic peaks at ~160°C. In addition to the endothermic peak, metronidazole has also shown an exothermic peak at ~274°C. In this regard, we have conducted the DSC analysis of drug containing microparticles up to 300°C. Thermal profiles of the drug containing microparticles are similar to their corresponding microparticles without drugs. Characteristic peaks corresponding to the drugs

have not been noticed in the thermograms of the microparticles. This suggests that the drugs are molecularly dispersed in the matrix of the microparticles (24).

Biocompatibility and Physical Interaction Studies

Biocompatibility of the microparticles was determined by studying the relative proliferation of MG63 cells in the presence of the microparticles extracts. The cell proliferation was measured using MTT assay. The results indicated that the cell viability index in the presence of the leachates of the microparticles was either ~1 or better than 1 indicating the biocompatible nature of the microparticles (Fig. 6a). The change in cell viability index was found to be insignificant with respect to control. The level of significance ($p < 0.05$) was calculated by using paired t test analysis (MS excel-2010).

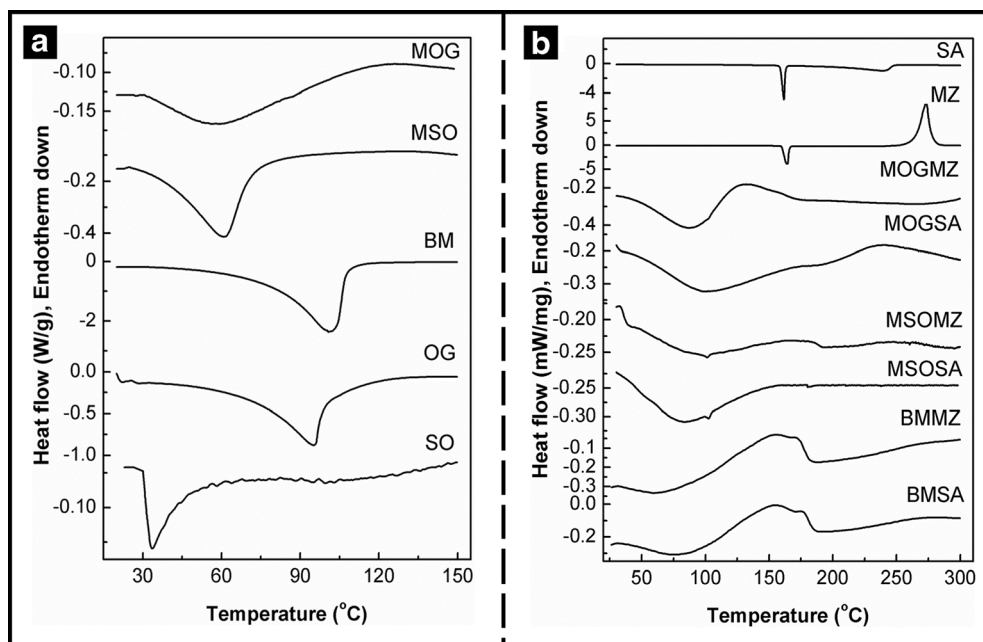Physical interaction of microparticles with mucous membrane was studied by *in vitro* wash-off method (Fig. 6b). In

Fig. 5. DSC thermograms of the **a** organogel and microparticles; **b** drugs and drug containing microparticles

general, alginate constructs possess high affinity toward intestinal mucosal layer. Under the experimental conditions, MSO detached quicker than MOG and BM. This may be accounted to the leaching of sunflower oil from MSO which was evident from the leaching studies. The mucoadhesive time of MOG was increased almost by sevenfold as compared to that of MSO. This is due to the prevention of oil leaching from MOG, due to the gelation of the internal phase. The differences in mucoadhesivity of microparticles were found to be significant ($p > 0.05$) as per paired t test analysis. The significant rise in the mucoadhesive nature of MOG is self-explanatory about the importance of the structuring of the edible oil within the microparticles. The results suggested that MOG may be tried as mucoadhesive microparticulate delivery vehicle.

In Vitro Drug-Release Studies

Figure 7 shows the *in vitro* cumulative percentage drug-release (CPDR) profiles of salicylic acid and metronidazole under gastric and intestinal conditions. The release of the drugs from the microparticles was affected by the pH of the dissolution medium. The drug release from BMSA/BMMZ and MSOSA/MSOMZ was lower than that from MOGSA/MOGMZ. This may be associated with the higher encapsulation efficiency of the drugs in MOGSA/MOGMZ as compared to that in BMSA/BMMZ and MSOSA/MSOMZ. As the leaching of the drug was higher in BMSA/BMMZ and MSOSA/MSOMZ, the percentage drug release from these microparticles was lower. Under gastric conditions, more metronidazole was released as compared to salicylic acid. On the other hand, a reverse trend was observed under intestinal conditions. The drug solubility under different pH conditions might also have affected their release pattern. Salicylic acid tends to be less soluble at low pH and more soluble at high pH due to its weak acidic nature (25). On the other hand, metronidazole has high solubility at low pH than at high pH (26).

The drug-release kinetics was studied by finding the best-fit release model after fitting in zero-order, first-order, Higuchi, and Baker-Lonsdale models. The diffusion of the drugs was figured
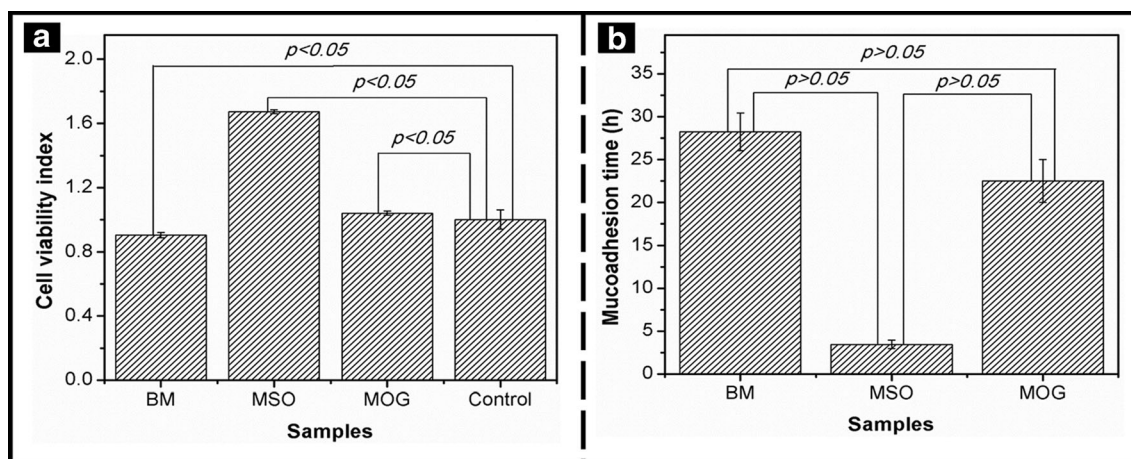

Fig. 6. **a** Biocompatibility and **b** mucoadhesion times of microparticles

out by calculating "*n*" value using Korsmeyer-Peppas model. The acceptable regression coefficient for fitting of the models was >0.95, and the best-fit models have been tabulated in Table III and shown in Fig. S1 (Supplementary File). By using the fit and observed values of the drug release, goodness-of-fit evaluations were performed using chi-square (χ^2) test. The obtained χ^2 values were found to be less than the critical χ^2 values (Table S1) (critical value of χ^2=32.671 at 21° of freedom). The χ^2 test indicated that the difference between the observed and expected values is statistically insignificant at α=0.05. The results suggested that the drug release from the microparticles followed Higuchian and Baker-Lonsdale kinetic models, indicating that the developed microparticles were swollen spherical matrix type (27). Under intestinal conditions, swelling
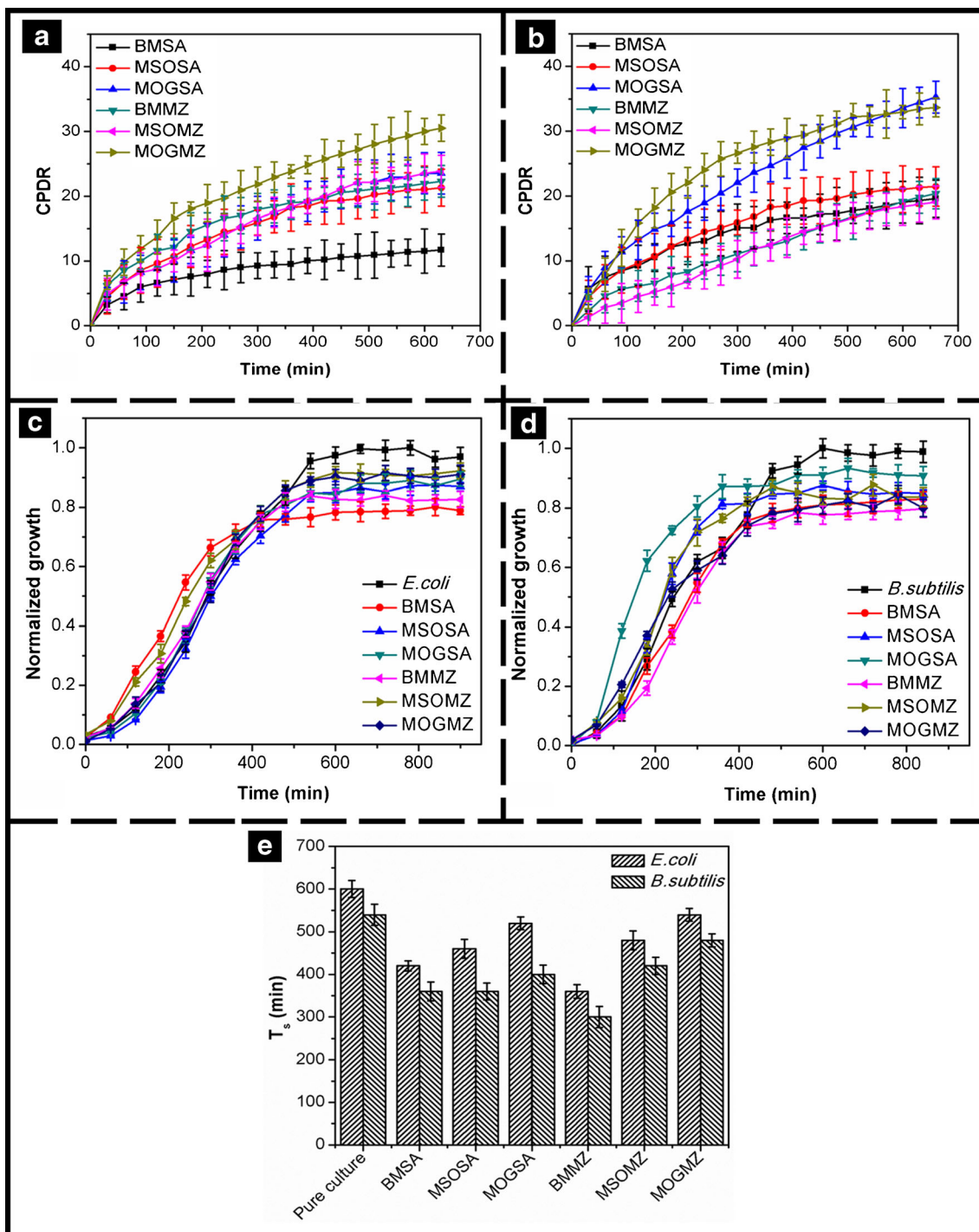

Fig. 7. *In vitro* drug release studies. CPDR profiles from microparticles: **a** in gastric buffer and **b** in intestinal buffer; antimicrobial activity of microparticles against **c** *E. coli* and **d** *B. subtilis*; and **e** time required to attain stationary phase in presence of microparticles

of microparticles facilitated the diffusion of the drugs from the microparticles. But under acidic conditions, the diffusion of the drugs was lower. This may be associated with the higher swelling of the microparticles under intestinal conditions and a lower swelling of the microparticles under acidic conditions (28). This phenomenon resulted in the release of the lower amount of the drugs under acidic conditions. Under intestinal conditions, erosion of the microparticles might also have contributed to the higher percentage releases, as was evident from the swelling and erosion studies (Supplementary File) (29). The release behavior of the drugs from BMSA/BMMZ followed Fickian diffusion under gastric conditions, whereas MSOSA/MSOMZ and MOGSA/MOGMZ followed non-Fickian diffusion. All the microparticles followed non-Fickian diffusion under intestinal conditions. The non-Fickian diffusion of the drugs may be attributed to the polymer relaxation, erosion, and degradation (29).

The results of the antimicrobial test by direct contact assay were compared with the growth curve of the pure bacterial culture (Fig. 7c, d). The antimicrobial activity was estimated by determining the time required for the bacteria to reach the stationary phase. If the bacteria reach stationary phase in lesser time as compared to the control, the microparticles are said to elicit antimicrobial action. The time required for reaching the stationary phase (T_s) of the bacteria against different microparticles has been shown in Fig. 7e.

The drug containing microparticles have shown considerable antimicrobial activity thereby suggesting that the incorporated drugs were bioactive even after encapsulation. MSOSA/MSOMZ microparticles have shown lower T_s (higher antimicrobial action) as compared to MOGSA/MOGMZ. This may be attributed to the quick release of the drugs from MSOSA/MSOMZ microparticles. The results showed absence of sudden stationary phases. This indicated that there was no burst release of the drugs from the microparticles. Similar results were also evident from the *in vitro* drug release. The results suggested that the organogels containing microparticles may be tried for the controlled delivery applications.

CONCLUSION

Encapsulation of the organogels prevented leaching of the internal phase of the microparticles, a common phenomenon when oil is encapsulated. The encapsulation efficiency of the drugs was improved after the encapsulation of organogels. The mucoadhesivity of the microparticles was improved by many-fold when the oil was encapsulated *via* organogel. Based on the preliminary results, the developed organogel containing microparticles are best suited to prevent the leakage of the internal phase and controlled delivery applications.

ACKNOWLEDGMENTS

REFERENCES

1. Chan LW, Lee HY, Heng PWS. Production of alginate microspheres by internal gelation using an emulsification method. Int J Pharm. 2002;242(1–2):259–62. doi:10.1016/S0378-5173(02)00170-9.
2. Sansone F, Mencherini T, Picerno P, d'Amore M, Aquino RP, Lauro MR. Maltodextrin/pectin microparticles by spray drying as carrier for nutraceutical extracts. J Food Eng. 2011;105(3):468–76.
3. Sansukcharearnpon A, Wanichwecharungruang S, Leepipatpaiboon N, Kerdcharoen T, Arayachukeat S. High loading fragrance encapsulation based on a polymer-blend: preparation and release behavior. Int J Pharm. 2010;391(1):267–73.
4. Cocero MJ, Martín Á, Mattea F, Varona S. Encapsulation and co-precipitation processes with supercritical fluids: fundamentals and applications. J Supercrit Fluids. 2009;47(3):546–55.
5. Sagiri SS, Behera B, Sudheep T, Pal K. Effect of composition on the properties of tween-80–span-80-based organogels. Des Monomers Polym. 2012;15(3):253–73. doi:10.1163/156855511X615669.
6. Pouton CW, Porter CJ. Formulation of lipid-based delivery systems for oral administration: materials, methods and strategies. Adv Drug Deliv Rev. 2008;60(6):625–37.
7. Peshkovsky AS, Peshkovsky SL, Bystryak S. Scalable high-power ultrasonic technology for the production of translucent nanoemulsions. Chem Eng Process Process Intensif. 2013;69:77–82.
8. Sagiri SS, Sethy J, Pal K, Banerjee I, Pramanik K, Maiti TK. Encapsulation of vegetable organogels for controlled delivery applications. Des Monomers Polym. 2012;16(4):366–376. doi:10.1080/15685551.2012.747154.
9. Simonoska Crcarevska M, Glavas Dodov M, Goracinova K. Chitosan coated Ca–alginate microparticles loaded with budesonide for delivery to the inflamed colonic mucosa. Eur J Pharm Biopharm. 2008;68(3):565–78. doi:10.1016/j.ejpb.2007.06.007.
10. Bordenave N, Janaswamy S, Yao Y. Influence of glucan structure on the swelling and leaching properties of starch microparticles. Carbohydr Polym. 2014;103:234–43.
11. Kulkarni AR, Soppimath KS, Aminabhavi TM, Rudzinski WE. In-vitro release kinetics of cefadroxil-loaded sodium alginate interpenetrating network beads. Eur J Pharm Biopharm. 2001;51(2):127–33.
12. Meerloo J, Kaspers GL, Cloos J. Cell sensitivity assays: the MTT assay. In: Cree IA, editor. Cancer cell culture. Humana Press; 2011. p. 237–45.
13. Martins S, Sarmento B, Souto EB, Ferreira DC. Insulin-loaded alginate microspheres for oral delivery—effect of polysaccharide reinforcement on physicochemical properties and release profile. Carbohydr Polym. 2007;69(4):725–31. doi:10.1016/j.carbpol.2007.02.012.
14. Gavini E, Sanna V, Sharma R, Juliano C, Usai M, Marchetti M, *et al*. Solid lipid microparticles (SLM) containing juniper oil as anti-acne topical carriers: preliminary studies. Pharm Dev Technol. 2005;10(4):479–87. doi:10.1080/10837450500299727.
15. Maji TK, Baruah I, Dube S, Hussain MR. Microencapsulation of *Zanthoxylum limonella* oil (ZLO) in glutaraldehyde crosslinked gelatin for mosquito repellent application. Bioresour Technol. 2007;98(4):840–4. doi:10.1016/j.biortech.2006.03.005.
16. Behera B, Sagiri SS, Pal K, Srivastava A. Modulating the physical properties of sunflower oil and sorbitan monopalmitate-based organogels. J Appl Polym Sci. 2013;127(6):4910–7.
17. Parashar BN, Mittal R. Elements of manufacturing processes. New Delhi: PHI Learning Pvt, Ltd.; 2002.

18. Dong Z, Wang Q, Du Y. Alginate/gelatin blend films and their properties for drug controlled release. J Membr Sci. 2006;280(1–2):37–44.

19. Tam SK, Dusseault J, Polizu S, Ménard M, Hallé J-P, Yahia LH. Physicochemical model of alginate–poly-l-lysine microcapsules defined at the micrometric/nanometric scale using ATR-FTIR, XPS, and ToF-SIMS. Biomaterials. 2005;26(34):6950–61.

20. Jia-hui Y, Yu-min D, Hua Z. Blend films of chitosan-gelatin. Wuhan Univ J Nat Sci. 1999;4(4):476.

21. Coates J. Interpretation of infrared spectra, a practical approach. Encyclopedia of analytical chemistry. Chichester: Wiley; 2006.

22. Vaidya A, Jain S, Agrawal RK, Jain SK. Pectin–metronidazole prodrug bearing microspheres for colon targeting. J Saudi Chem Soc. doi:10.1016/j.jscs.2012.03.001.

23. Suzuki M, Nakajima Y, Yumoto M, Kimura M, Shirai H, Hanabusa K. Effects of hydrogen bonding and van der Waals interactions on organogelation using designed low-molecular-weight gelators and gel formation at room temperature. Langmuir. 2003;19(21):8622–4.

24. Ramesh Babu V, Sairam M, Hosamani KM, Aminabhavi TM. Preparation of sodium alginate–methylcellulose blend microspheres for controlled release of nifedipine. Carbohydr Polym. 2007;69(2):241–50.

25. Ostrowska-Czubenko J, Gierszewska-Drużyńska M. Effect of ionic crosslinking on the water state in hydrogel chitosan membranes. Carbohydr Polym. 2009;77(3):590–8.

26. Yamashita S, Kataoka M, Higashino H, Sakuma S, Sakamoto T, Uchimaru H, *et al.* Measurement of drug concentration in the stomach after intragastric administration of drug solution to healthy volunteers: analysis of intragastric fluid dynamics and drug absorption. Pharm Res. 2013;30(4):951–958.

27. Radin S, Chen T, Ducheyne P. The controlled release of drugs from emulsified, sol gel processed silica microspheres. Biomaterials. 2009;30(5):850–8.

28. Cui J-H, Goh J-S, Kim P-H, Choi S-H, Lee B-J. Survival and stability of bifidobacteria loaded in alginate poly-l-lysine microparticles. Int J Pharm. 2000;210(1–2):51–9.

29. Pasparakis G, Bouropoulos N. Swelling studies and in vitro release of verapamil from calcium alginate and calcium alginate–chitosan beads. Int J Pharm. 2006;323(1–2):34–42. doi:10.1016/j.ijpharm.2006.05.054.